

## Optimizing Performance of Quantum Operations with Non-Markovian Decoherence: The Tortoise or the Hare?

Eoin P. Butler<sup>1,2</sup>, Gerald E. Fux<sup>3,4</sup>, Carlos Ortega-Taberner<sup>1,2</sup>, Brendon W. Lovett<sup>3</sup>,  
Jonathan Keeling<sup>3</sup> and Paul R. Eastham<sup>1,2</sup>

<sup>1</sup>*School of Physics, Trinity College Dublin, College Green, Dublin 2, Ireland*

<sup>2</sup>*Trinity Quantum Alliance, Unit 16, Trinity Technology and Enterprise Centre, Pearse Street, Dublin 2, Ireland*

<sup>3</sup>*SUPA, School of Physics and Astronomy, University of St Andrews, St Andrews KY16 9SS, United Kingdom*

<sup>4</sup>*Abdus Salam International Center for Theoretical Physics (ICTP), Strada Costiera 11, 34151 Trieste, Italy*



(Received 28 April 2023; accepted 19 December 2023; published 8 February 2024)

The interaction between a quantum system and its environment limits our ability to control it and perform quantum operations on it. We present an efficient method to find optimal controls for quantum systems coupled to non-Markovian environments, by using the process tensor to compute the gradient of an objective function. We consider state transfer for a driven two-level system coupled to a bosonic environment, and characterize performance in terms of speed and fidelity. This allows us to determine the best achievable fidelity as a function of process duration. We show there can be a trade-off between speed and fidelity, and that slower processes can have higher fidelity by exploiting non-Markovian effects.

DOI: [10.1103/PhysRevLett.132.060401](https://doi.org/10.1103/PhysRevLett.132.060401)

The control of quantum systems using time-dependent Hamiltonians is crucial for quantum technologies [1], enabling the implementation of state transfer and gate operations. An important task is to establish how optimal performance can be achieved for such processes. In an ideal closed quantum system perfect operations are possible given sufficient time [2]. A speed limit arises because physical Hamiltonians are bounded, so that energy-time uncertainty gives a maximum rate of time evolution and hence a minimum operation time. Beyond this ideal case, however, other considerations arise. One is a desire for reliable operation when precise control cannot be guaranteed; this can be achieved by using robust control techniques [3] or adiabatic processes [4,5]. Another is the impact of decoherence and dissipation. In the standard Markovian approximation such processes give a cumulative loss of information with time. Thus, one generally expects fast operation to be desirable to minimize information loss, although there are notable exceptions, where slower operation allows access to a decoherence-free subspace [6]. In this Letter, we show that fast operation is not always desirable in non-Markovian systems, because slower operation can enable information backflow to be harnessed to increase fidelity.

To provide a concrete demonstration of the trade-off between speed and fidelity in non-Markovian systems we use numerical optimal control to explore the achievable performance for a system consisting of a driven qubit interacting with a bosonic environment. Optimal control [7] involves determining a set of time-dependent control fields that maximize an objective function such as the fidelity. Here, we show that this can be done effectively in a

non-Markovian system, using an extension of our previously introduced process tensor approach [8] to efficiently compute the gradient of the objective function. This allows us to repeatedly optimize over many hundreds of control parameters for different process durations, and so find the achievable fidelity as a function of the process duration. Our results reveal a marked improvement in fidelity for process durations  $T$  longer than a value  $T_0$ , set by the speed limit in the closed system [2]. We further compute a widely used measure of non-Markovianity, based on trace distance [9], and show that the improved fidelity coincides with an increase in non-Markovianity. Since many types of devices exhibit regimes of non-Markovian decoherence our results could enable performance improvements across a range of quantum technologies [10], including superconducting circuits [11,12], spins [13], quantum dots [8,14], color centers in diamond [15], and cold atoms [16–18].

Our approach applies to an open quantum system comprising a few-state system Hamiltonian  $H_S$  interacting with an environment (bath) with Hamiltonian  $H_B$  through a coupling  $H_{SB}$ . Models of this form are typically treated under the assumptions of weak system-bath coupling and short bath correlation time (Born-Markov). This implies that information about the system only flows away into the environment, and does not return, leading to simple time-local evolution equations for the system reduced density matrix  $\rho_S$  [19]. To avoid making these approximations we use process tensors (PT), which are general objects that encode the complete influence of the environment. Our approach applies to any open quantum system for which the PT can be computed as a matrix product operator with low bond dimension.

Time-local evolution equations for  $\rho_S$  have been used to explore performance limits [20–22] using optimal control [23] in various problems. Studying optimal control beyond their applicability has so far been difficult. One approach is to expand the system to incorporate a few modes of the environment, which are then treated exactly, with the remaining environment modes providing Markovian damping. This approach has been used to study controllability [24], optimal control [25,26], and speed limits [22]. However, it becomes intractable when one considers more than a few modes of the environment. Another method involves computing the time-local dissipator describing non-Markovian dynamics using lowest-order perturbation theory [27] or the hierarchical equations of motion [28]. These techniques have been used within optimal control to demonstrate fidelity increases, and can be effective when the environment spectral density can be approximated by a small number of Lorentzians. Another type of approach [29] uses the stochastic Liouville equation, but is limited by the need to average over a large and *a priori* unknown number of trajectories. Some works [30–32] have obtained optimal protocols under the assumption that the dissipation is described by a fixed time-local dissipator, such as that for a pure dephasing channel [33,34]. An issue, however, is that for optimal control one must consider the effect of the time-dependent control fields on the dissipative processes [35].

To overcome these challenges, we extend the process tensor method described in our previous work [8] for solving the dynamics of non-Markovian open systems. The process tensor [36,37] is a multilinear map from the set of all possible system control operation sequences to the resulting output states, constructed by discretizing the time evolution into a series of time steps. It can often be computed in matrix-product operator form with low bond dimension using algorithms that systematically discard irrelevant correlations [39,40]. For a Gaussian bosonic environment efficient representations can be found using the methods introduced in [8,41–44], which are often effective for smooth spectral densities. A range of methods for bosonic, fermionic, and spin environments is now available [45–56]. Once computed, the PT can be contracted to time-evolve  $\rho_S$  for any  $H_S$ , as shown in Fig. 1(a). In this tensor network diagram [40] each node represents a tensor, each leg represents an index, and connections between legs correspond to contractions. The diagram is in Liouville space so that operators such as  $\rho_S$  are rank-1 objects (i.e., objects with a single index), and maps between operators, such as the propagators across each time step  $U_t = e^{\Delta t \mathcal{L}_S(t)}$  with  $\mathcal{L}_S(t) \bullet = -i[H_S(t), \bullet]$ , are rank-2. The PT is the region in the dashed box, which can be contracted with an initial density matrix and the Trotterized propagators [57] to obtain  $\rho_S$  at later times.

For optimal control we must define an objective function. In the following we consider the example of a state

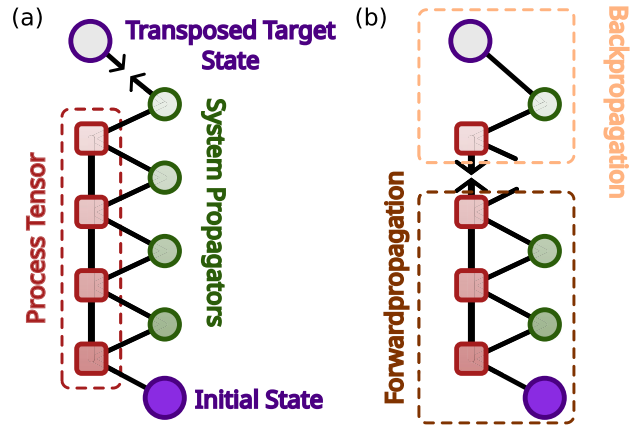


FIG. 1. (a) Tensor network representation of the propagation of an initial state over four time steps and calculation of the fidelity. Time increases going up the diagram. The evolved density matrix is given by this diagram without the target state node. The fidelity is obtained by joining the legs indicated by arrows. (b) The derivative of the fidelity with respect to the penultimate propagator is given by joining the legs indicated by the arrows, contracting a pair of indices in the product of one tensor formed during a forward propagation with one formed during a backward propagation.

transfer process, for which we use the fidelity  $\mathcal{F}$  [58] between the desired target state and the obtained final state  $\rho_f = \rho_S(t_f)$ . To simplify the presentation of the method we assume a pure target state, with density matrix  $\sigma = |\sigma\rangle\langle\sigma|$ , in which case  $\mathcal{F} = \langle\sigma|\rho_f|\sigma\rangle$  is a linear function of the final state. In Liouville space it is the scalar product of the vectors representing the final density matrix and the transposed target density matrix, corresponding to the diagram in Fig. 1(a). The generalization of the method to nonlinear objective functions, such as the fidelity for a mixed target state, is straightforward [37].

An optimal protocol is found by numerically maximizing  $\mathcal{F}$  over  $N$  control parameters that determine the system propagators at each discrete time step. Such numerical optimization becomes significantly faster if one can efficiently calculate the gradient of  $\mathcal{F}$  with respect to the  $N$ -dimensional vector of control parameters,  $\nabla\mathcal{F}$ . A naive calculation of  $\nabla\mathcal{F}$  requires of order  $N$  evaluations of  $\mathcal{F}$ , strongly limiting the size of problems that can be treated. Such gradients can, however, be efficiently obtained using the adjoint method [59], which has been applied to unitary or Markovian dynamics [60,61]. In the GRAPE algorithm [60], for example, the gradient is computed by combining states stored during a forward-in-time propagation from the initial state with those stored during a backward-in-time propagation from the target state. Crucially, one may see that the tensor network representation of  $\mathcal{F}$  in Fig. 1(a) leads immediately to the generalization required for non-Markovian dynamics. This diagram represents the fidelity as a multilinear functional of the propagators; thus the derivative with respect to the propagator at a given time step

is the same diagram with the node for that propagator removed. As shown in Fig. 1(b), and discussed further in [37], all such derivatives can be computed by combining rank-2 tensors stored as the network is evaluated forward in time with those stored during a backward propagation. The key difference compared to the adjoint method for unitary or Markovian dynamics is that we propagate a rank-2 tensor rather than the state  $\rho_S$ . The additional index in this tensor encodes information about the past and future dynamics and enables optimization of non-Markovian evolutions.

To illustrate the general principle, we consider an example of optimal state transfer in a driven two-level system. Our system Hamiltonian is  $H_S = h_x(t)s_x + h_z(t)s_z$ , where the fields  $h_{x,z}(t)$  are the controls. We treat them as piecewise constants with values  $h_{x,z}(t_n)$  at the time steps  $t_n = n\Delta t$ . We seek to determine the control fields that steer the state  $\rho_S(t)$  from a prescribed initial state to a target state. The bath is a set of harmonic oscillators, and the coupling is  $H_{SB} = s_z \sum_q (g_q b_q + g_q^* b_q^\dagger)$ . This model is known as the spin-boson model, and it describes many physical systems [62,63]. For definiteness, we take parameters appropriate for an optical transition on a quantum dot, driven by laser pulses [64]. In that case  $h_z$  is the difference between the transition frequency and the laser frequency, and  $h_x$  the signed Rabi frequency (obtained by writing the oscillating driving field in terms of its real-valued amplitude and frequency). In the quantum dot the bosonic modes are acoustic phonon modes, for which we use the super-Ohmic spectral density  $J(\omega) = 2\alpha\omega^3\omega_c^{-2} \exp[-\omega^2/\omega_c^2]$  with  $\alpha = 0.126$  and  $\omega_c = 3.04 \text{ ps}^{-1}$  [65,66], and use a bath temperature of 5 K. We take the initial and target states to be the eigenstates of  $s_x$  with eigenvalues  $\mp 1$  respectively. Note that this process differs from that usually emphasized for quantum dots [65,66], which is a transfer between eigenstates of  $s_z$ .

We have determined optimal controls  $h_x(t_n)$ ,  $h_z(t_n)$  by numerically maximizing  $\mathcal{F}$  using the limited-memory Broyden–Fletcher–Goldfarb–Shanno algorithm [67,68], with the gradient and fidelity computed with the PT. To explore the impact of speed on fidelity we perform this optimization for different process durations  $T$ , with bounds on the controls,  $|h_x| \leq h_x^{\max} = 5 \text{ ps}^{-1}$  and  $|h_z| \leq h_z^{\max} = 1 \text{ ps}^{-1}$ , to consider the realistic case in which the Hamiltonian, and therefore the speed of the unitary evolution, is restricted. We note that in the unitary case, the speed limit for state transfer has been identified from the rate of convergence of the Krotov algorithm [20]. Here, we consider a fully non-Markovian dissipative system, and use numerically converged optimization to identify the speed limit from the behavior of the fidelity against process duration. Figure 2(a) shows the resulting infidelity,  $1 - \mathcal{F}$  for this optimized protocol, which we refer to as “control A”.

It is interesting to compare the optimized results with those for the protocols that are optimal for unitary dynamics in the closed system [69], denoted “control B,” which

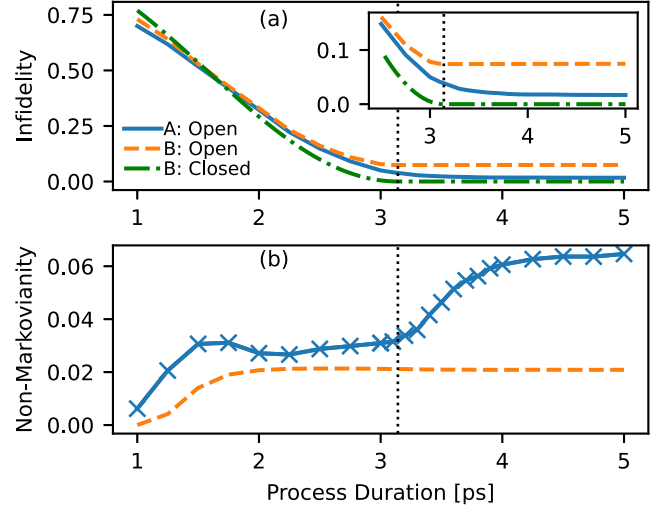


FIG. 2. (a) Infidelity,  $1 - \mathcal{F}$ , for state transfer as a function of process duration with bounded control fields. Results are shown for the optimal protocol of the non-Markovian spin-boson model (control A) and for driving with a constant field (control B). The latter is an optimal protocol in the closed system. Blue solid: infidelity of control A in the spin-boson model. Orange dashed: infidelity of control B in the spin-boson model. Green dash-dotted: infidelity of control B in the closed system. (b) Non-Markovianity measure as a function of process duration in the spin-boson model for controls A (blue solid) and B (orange dashed). The vertical dotted lines are the speed limit time  $T_0$  of the closed system.

we used as the starting point for the optimization. These protocols can be understood by noting that for unitary dynamics one can achieve the state transfer with infidelity zero by setting  $h_x = 0$  and choosing  $h_z(t)$  such that its time integral is  $\pi$ . Such a protocol is optimal if it satisfies the constraint  $|h_z(t)| < h_z^{\max}$  for all times, which is possible when  $T$  is greater than the speed limit time  $T_0 = \pi/h_z^{\max}$  (which saturates both the Mandelstam-Tamm and Margolus-Levitin bounds [2]). Among protocols satisfying the above condition, we choose  $h_z(t) = \pi/T$ . For  $T < T_0$  the state transfer is not fully achievable and the optimal protocol is that with  $h_z(t) = \pm h_z^{\max}$ . Thus, in both regimes, we have an optimal protocol with a time-independent  $H_S$ . As can be seen in Fig. 2(a), the infidelity of this protocol (control B) for the unitary dynamics smoothly decreases as the duration  $T$  increases from zero, before saturating at zero for  $T > T_0$ . Applying this same protocol in the open system gives a similar overall behavior, with the key difference being that the saturated value of the infidelity at large  $T$  is now nonzero. This behavior differs from that obtained for this control in a Markovian model with a constant decoherence rate, where slower processes produce higher infidelity, i.e., growing with  $T$ . In the “control B” protocol, we have  $h_z(t) = h_z$  and  $h_x = 0$ , so that the model is the exactly solvable independent-boson model [70,71], which has non-Markovian decoherence. The constant infidelity

for  $T > T_0$  comes from the decoherence function of the independent-boson model, which approaches a nonzero constant for times  $T \gg \tau_b \sim 1/\omega_c$ .

Figure 2 shows that the optimization increases the performance for all process durations, as one would expect, but the increase becomes marked when  $T > T_0$ . This is because the fidelity in this regime is limited not by the distance to the target state and the speed of unitary evolution under  $H_S$ , but by the decoherence and dissipation produced by the bath. The improved fidelity thus corresponds to suppressing decoherence.

An approach to suppressing decoherence one might consider is dynamical decoupling [71] (DD). Such a protocol uses control fields to produce dynamics for the system that averages away the effects of the bath, which requires that the timescale of the system is much shorter than that of the bath  $\tau_b$ . This regime is not accessible in our optimization due to the bounds on the controls. The standard DD sequence for the process we consider would be a train of  $\pi$  pulses separated by a time  $\tau \ll \tau_b$  and each with duration  $\tau_p \ll \tau$ ; this would produce rapid spin flips and so average away  $H_{SB} \propto s_z$ . Thus, standard DD requires  $|h_x| \gg \pi/\tau_b$ , which with  $\tau_b \sim 1/\omega_c \sim 0.3$  ps is greater than  $h_x^{\max}$ .

To explore the mechanism that is giving the improvement in fidelity we compute a measure of non-Markovianity. There are many such interrelated measures [63,72,73] including, among others, those based on divisibility and complete positivity, and those based on information backflow. We choose that introduced by Breuer, Lane, and Piilo [9], formed from the trace distance between pairs of states  $D_{12} = \text{Tr}|\rho_1(t) - \rho_2(t)|/2$ , where  $\rho_1(t)$  and  $\rho_2(t)$  are obtained by time-evolving initial states  $\rho_1$  and  $\rho_2$ , respectively. The non-Markovianity is

$$\mathcal{N} = \max_{\rho_1, \rho_2} \int \frac{dD_{12}}{dt} dt, \quad (1)$$

where the integral extends over regions where the integrand is positive, and the maximum is over all pairs of orthogonal states on the surface of the Bloch sphere (which is the same as the maximum over all pairs of initial states; see [74]). The two curves in Fig. 2(b) show the non-Markovianity as a function of process duration for the optimal controls (solid) and the constant field (dashed). For control B, the non-Markovianity increases from zero as the process duration increases from zero, becoming constant for  $T \gtrsim 2$  ps. This corresponds to the buildup of correlations due to the system-bath coupling in the independent-boson model, and is unaffected by the system dynamics since  $[H_S, H_{SB}] = 0$  when  $h_x = 0$ . The non-Markovianity with the optimal control A is higher, but initially shows a similar increase and saturation as the duration  $T$  increases from zero. However, there is then a marked feature at  $T \approx T_0$ , beyond which the non-Markovianity increases rapidly with

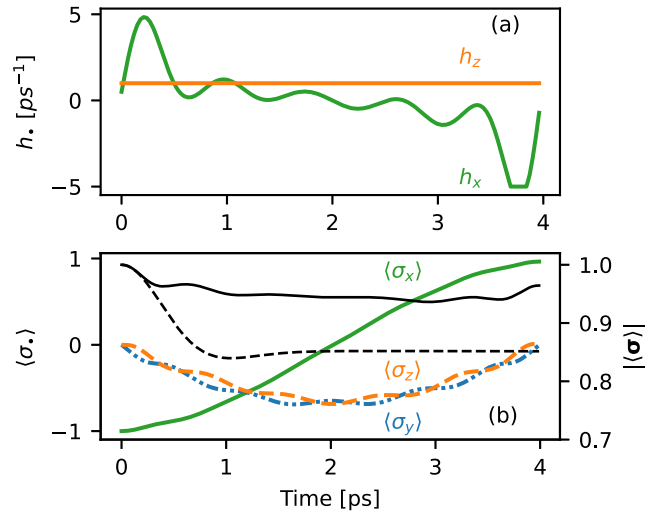


FIG. 3. (a) Driving fields  $h_x(t)$  (green) and  $h_z(t)$  (orange) for the optimal state transfer process, control A, of duration 4.0 ps. (b) Dynamics of the components of the Bloch vector (left axis, green solid,  $\langle \sigma_x \rangle$ ; blue dot-dashed,  $\langle \sigma_y \rangle$ ; orange dashed,  $\langle \sigma_z \rangle$ ) and length of the Bloch vector (right axis, black solid). The length of the Bloch vector for control B is also shown (right axis, black dashed).

process duration before reaching a new and much higher level. This suggests that the improvement in fidelity for long process durations occurs because the optimization increases the degree of non-Markovianity of the map, restoring some of the information lost to the environment during the earlier parts of the dynamics by the end of the process.

Figure 3 shows the optimized controls (top panel), and the dynamics of the Bloch vector  $\langle \sigma_{x,y,z} \rangle$ , for the optimal protocol, control A, at  $T = 4.0$  ps. For this duration, the optimal  $h_z$  remains constant, while the optimized  $h_x$  has an overall slope and oscillations of varying magnitude. The resulting dynamics of the Bloch vector moves down below the equator during the control and develops weak oscillations. The clearest effect of the optimization is seen in the length of the Bloch vector, which is shown for both protocols A and B. In the latter case the length of the Bloch vector is given by the decoherence function of the independent-boson model, which goes from one, for zero time, to a constant nonzero value at late times. The optimal control A clearly avoids this decay and even shows an increase in the Bloch-vector length at the very end of the pulse, consistent with a decoherence suppression mechanism. The control in  $h_x$  is very different from that for a standard DD sequence as described above. The behavior shown is representative of that we find for other process durations [37]. For a unitary dynamics it has been shown that there is a unique global optimum for durations near the quantum speed limit [75]. The consistency in the form of our solutions suggests that this may also be the case here.

Some insight into a possible mechanism for the improved fidelity can be gained by considering the

decoherence at zero temperature when  $h_x = h_z = 0$ . This is the solvable independent-boson model [70,71], in which an initial product state  $|\uparrow_x\rangle \otimes |0\rangle = (|\uparrow\rangle + |\downarrow\rangle) \otimes |0\rangle/\sqrt{2}$  evolves to  $(|\uparrow\rangle \otimes |f\rangle + |\downarrow\rangle \otimes |-f\rangle)/\sqrt{2}$ . Here,  $|\pm f\rangle$  are bath states in which the Gaussian ground-state wave functions of the oscillators have evolved in oppositely displaced potentials. This reduces the system coherence by the overlap of the bath states,  $\langle\sigma_x\rangle = 2\text{Re}\langle f|-f\rangle$ . We suggest that our controls both suppress and reverse this polaron formation process, disentangling the system and environment. For a single-oscillator environment such disentangling occurs periodically without the control fields; our optimization may be exploiting similar physics in an ensemble. Optimization results for other spectral densities and temperatures [37] are consistent with this suggestion.

In conclusion, we have presented a method for computing optimal controls in general non-Markovian systems. It extends the PT method [8] to efficiently compute gradients, so permitting optimization over large numbers of control parameters. The method takes full account of the changes in the dissipator produced by the control fields, allowing it to discover protocols that exploit non-Markovianity for improved performance. We have used it to investigate state transfer in the spin-boson model, where we find that slow processes can improve on fast ones by exploiting non-Markovian effects. These results show that performance improvements are possible across the many qubit implementations subject to non-Markovian decoherence, and could be identified using the methods described here.

The supporting data for this article are openly available from Zenodo [76].

We acknowledge discussions with F. Binder. E. P. B. acknowledges support from the Irish Research Council (GOIPG/2019/1871). G. E. F. acknowledges support from EPSRC (EP/L015110/1). B. W. L. and J. K. acknowledge support from EPSRC (EP/T014032/1). P. R. E. acknowledges support from Science Foundation Ireland (21/FFP-P/10142).

---

[1] S. J. Glaser, U. Boscain, T. Calarco, C. P. Koch, W. Köckenberger, R. Kosloff, I. Kuprov, B. Luy, S. Schirmer, T. Schulte-Herbrüggen, D. Sugny, and F. K. Wilhelm, Training Schrödinger's cat: Quantum optimal control, *Eur. Phys. J. D* **69**, 279 (2015).

[2] S. Deffner and S. Campbell, Quantum speed limits: From Heisenberg's uncertainty principle to optimal quantum control, *J. Phys. A* **50**, 453001 (2017).

[3] T. Propson, B. E. Jackson, J. Koch, Z. Manchester, and D. I. Schuster, Robust quantum optimal control with trajectory optimization, *Phys. Rev. Appl.* **17**, 014036 (2022).

[4] A. Benseny and K. Mølmer, Adiabatic theorem revisited: The unexpectedly good performance of adiabatic passage, *Phys. Rev. A* **103**, 062215 (2021).

[5] E. Torrontegui, S. Ibáñez, S. Martínez-Garaot, M. Modugno, A. del Campo, D. Guéry-Odelin, A. Ruschhaupt, X. Chen, and J. G. Muga, Shortcuts to adiabaticity, in *Advances in Atomic, Molecular, and Optical Physics*, edited by E. Arimondo, P. R. Berman, and C. C. Lin (Academic Press, New York, 2013), Vol. 62, pp. 117–169.

[6] D. Basilewitsch, H. Yuan, and C. P. Koch, Optimally controlled quantum discrimination and estimation, *Phys. Rev. Res.* **2**, 033396 (2020).

[7] C. P. Koch, U. Boscain, T. Calarco, G. Dirr, S. Filipp, S. J. Glaser, R. Kosloff, S. Montangero, T. Schulte-Herbrüggen, D. Sugny, and F. K. Wilhelm, Quantum optimal control in quantum technologies. Strategic report on current status, visions and goals for research in Europe, *Eur. Phys. J. Quantum Technol.* **9**, 19 (2022).

[8] G. E. Fux, E. P. Butler, P. R. Eastham, B. W. Lovett, and J. Keeling, Efficient exploration of Hamiltonian parameter space for optimal control of non-Markovian open quantum systems, *Phys. Rev. Lett.* **126**, 200401 (2021).

[9] E.-M. Laine, J. Piilo, and H.-P. Breuer, Measure for the non-Markovianity of quantum processes, *Phys. Rev. A* **81**, 062115 (2010).

[10] A. Acín, I. Bloch, H. Buhrman, T. Calarco, C. Eichler, J. Eisert, D. Esteve, N. Gisin, S. J. Glaser, F. Jelezko, S. Kuhr, M. Lewenstein, M. F. Riedel, P. O. Schmidt, R. Thew, A. Wallraff, I. Walmsley, and F. K. Wilhelm, The quantum technologies roadmap: A European community view, *New J. Phys.* **20**, 080201 (2018).

[11] J. Fischer, D. Basilewitsch, C. P. Koch, and D. Sugny, Time-optimal control of the purification of a qubit in contact with a structured environment, *Phys. Rev. A* **99**, 033410 (2019).

[12] M. H. Goerz, F. Motzoi, K. B. Whaley, and C. P. Koch, Charting the circuit QED design landscape using optimal control theory, *npj Quantum Inf.* **3**, 37 (2017).

[13] F. Dolde, V. Bergholm, Y. Wang, I. Jakobi, B. Naydenov, S. Pezzagna, J. Meijer, F. Jelezko, P. Neumann, T. Schulte-Herbrüggen, J. Biamonte, and J. Wrachtrup, High-fidelity spin entanglement using optimal control, *Nat. Commun.* **5**, 3371 (2014).

[14] I. Wilson-Rae and A. Imamoglu, Quantum dot cavity-QED in the presence of strong electron-phonon interactions, *Phys. Rev. B* **65**, 235311 (2002).

[15] A. Norambuena, J. R. Maze, P. Rabl, and R. Coto, Quantifying phonon-induced non-Markovianity in color centers in diamond, *Phys. Rev. A* **101**, 022110 (2020).

[16] T. Choi, S. Debnath, T. A. Manning, C. Figgatt, Z.-X. Gong, L.-M. Duan, and C. Monroe, Optimal quantum control of multimode couplings between trapped ion qubits for scalable entanglement, *Phys. Rev. Lett.* **112**, 190502 (2014).

[17] M. G. Bason, M. Viteau, N. Malossi, P. Huillery, E. Arimondo, D. Ciampini, R. Fazio, V. Giovannetti, R. Mannella, and O. Morsch, High-fidelity quantum driving, *Nat. Phys.* **8**, 147 (2012).

[18] P. Treutlein, T. W. Hänsch, J. Reichel, A. Negretti, M. A. Cirone, and T. Calarco, Microwave potentials and optimal control for robust quantum gates on an atom chip, *Phys. Rev. A* **74**, 022312 (2006).

[19] H.-P. Breuer and F. Petruccione, *The Theory of Open Quantum Systems* (Oxford University Press, New York, 2007).

- [20] T. Caneva, M. Murphy, T. Calarco, R. Fazio, S. Montangero, V. Giovannetti, and G. E. Santoro, Optimal control at the quantum speed limit, *Phys. Rev. Lett.* **103**, 240501 (2009).
- [21] A. del Campo, I. L. Egusquiza, M. B. Plenio, and S. F. Huelga, Quantum speed limits in open system dynamics, *Phys. Rev. Lett.* **110**, 050403 (2013).
- [22] S. Deffner and E. Lutz, Quantum speed limit for non-Markovian dynamics, *Phys. Rev. Lett.* **111**, 010402 (2013).
- [23] C. P. Koch, Controlling open quantum systems: Tools, achievements, and limitations, *J. Phys. Condens. Matter* **28**, 213001 (2016).
- [24] D. M. Reich, N. Katz, and C. P. Koch, Exploiting non-Markovianity for quantum control, *Sci. Rep.* **5**, 12430 (2015).
- [25] P. Rebentrost, I. Serban, T. Schulte-Herbrüggen, and F. K. Wilhelm, Optimal control of a qubit coupled to a non-Markovian environment, *Phys. Rev. Lett.* **102**, 090401 (2009).
- [26] F. F. Floether, P. de Fouquieres, and S. G. Schirmer, Robust quantum gates for open systems via optimal control: Markovian versus non-Markovian dynamics, *New J. Phys.* **14**, 073023 (2012).
- [27] B. Hwang and H.-S. Goan, Optimal control for non-Markovian open quantum systems, *Phys. Rev. A* **85**, 032321 (2012).
- [28] E. Mangaud, R. Puthumpally-Joseph, D. Sugny, C. Meier, O. Atabek, and M. Desouter-Lecomte, Non-Markovianity in the optimal control of an open quantum system described by hierarchical equations of motion, *New J. Phys.* **20**, 043050 (2018).
- [29] R. Schmidt, A. Negretti, J. Ankerhold, T. Calarco, and J. T. Stockburger, Optimal control of open quantum systems: Cooperative effects of driving and dissipation, *Phys. Rev. Lett.* **107**, 130404 (2011).
- [30] Y. Ohtsuki, Non-Markovian effects on quantum optimal control of dissipative wave packet dynamics, *J. Chem. Phys.* **119**, 661 (2003).
- [31] J. Ying-Hua, H. Ju-ju, H. Jian-Hua, and K. Qiang, Optimal control-based states transfer for non-Markovian quantum system, *Physica (Amsterdam)* **81E**, 77 (2016).
- [32] W. Cui, Z. R. Xi, and Y. Pan, Optimal decoherence control in non-Markovian open dissipative quantum systems, *Phys. Rev. A* **77**, 032117 (2008).
- [33] A. W. Chin, S. F. Huelga, and M. B. Plenio, Quantum metrology in non-Markovian environments, *Phys. Rev. Lett.* **109**, 233601 (2012).
- [34] B. Bylicka, D. Chruściński, and S. Maniscalco, Non-Markovianity and reservoir memory of quantum channels: A quantum information theory perspective, *Sci. Rep.* **4**, 5720 (2014).
- [35] C. Addis, E.-M. Laine, C. Gneiting, and S. Maniscalco, Problem of coherent control in non-Markovian open quantum systems, *Phys. Rev. A* **94**, 052117 (2016).
- [36] F. A. Pollock, C. Rodríguez-Rosario, T. Frauenheim, M. Paternostro, and K. Modi, Non-Markovian quantum processes: Complete framework and efficient characterization, *Phys. Rev. A* **97**, 012127 (2018).
- [37] See Supplemental Material at <http://link.aps.org/supplemental/10.1103/PhysRevLett.132.060401>, which includes Ref. [38], for additional details of process tensors, the method for computation of gradients, and additional results.
- [38] F. Campaioli, F. A. Pollock, and K. Modi, Tight, robust, and feasible quantum speed limits for open dynamics, *Quantum* **3**, 168 (2019).
- [39] F. Verstraete, J. J. García-Ripoll, and J. I. Cirac, Matrix product density operators: Simulation of finite-temperature and dissipative systems, *Phys. Rev. Lett.* **93**, 207204 (2004).
- [40] R. Orús, A practical introduction to tensor networks: Matrix product states and projected entangled pair states, *Ann. Phys. (N.Y.)* **349**, 117 (2014).
- [41] N. Makri and D. E. Makarov, Tensor propagator for iterative quantum time evolution of reduced density matrices. II. Numerical methodology, *J. Chem. Phys.* **102**, 4611 (1995).
- [42] N. Makri and D. E. Makarov, Tensor propagator for iterative quantum time evolution of reduced density matrices. I. Theory, *J. Chem. Phys.* **102**, 4600 (1995).
- [43] A. Strathearn, P. Kirton, D. Kilda, J. Keeling, and B. W. Lovett, Efficient non-Markovian quantum dynamics using time-evolving matrix product operators, *Nat. Commun.* **9**, 3322 (2018).
- [44] M. R. Jørgensen and F. A. Pollock, Exploiting the causal tensor network structure of quantum processes to efficiently simulate non-Markovian path integrals, *Phys. Rev. Lett.* **123**, 240602 (2019).
- [45] M. C. Bañuls, M. B. Hastings, F. Verstraete, and J. I. Cirac, Matrix product states for dynamical simulation of infinite chains, *Phys. Rev. Lett.* **102**, 240603 (2009).
- [46] A. Strathearn, *Modelling Non-Markovian Quantum Systems Using Tensor Networks*, Springer Theses (Springer International Publishing, Cham, 2020), 10.1007/978-3-030-54975-6.
- [47] A. Lerose, M. Sonner, and D. A. Abanin, Influence matrix approach to many-body Floquet dynamics, *Phys. Rev. X* **11**, 021040 (2021).
- [48] M. Cygorek, M. Cosacchi, A. Vagov, V. M. Axt, B. W. Lovett, J. Keeling, and E. M. Gauger, Simulation of open quantum systems by automated compression of arbitrary environments, *Nat. Phys.* **18**, 662 (2022).
- [49] M. Sonner, A. Lerose, and D. A. Abanin, Influence functional of many-body systems: Temporal entanglement and matrix-product state representation, *Ann. Phys. (N.Y.)* **435**, 168677 (2021), special issue on Philip W. Anderson.
- [50] E. Ye and G. K.-L. Chan, Constructing tensor network influence functionals for general quantum dynamics, *J. Chem. Phys.* **155**, 044104 (2021).
- [51] G. White, F. Pollock, L. Hollenberg, K. Modi, and C. Hill, Non-Markovian quantum process tomography, *PRX Quantum* **3**, 020344 (2022).
- [52] J. Thoenniss, A. Lerose, and D. A. Abanin, Non-equilibrium quantum impurity problems via matrix-product states in the temporal domain, *Phys. Rev. B* **107**, 195101 (2023).
- [53] The TEMPO Collaboration, OQuPy: A Python3 package to efficiently compute non-Markovian open quantum systems, Zenodo: 10.5281/zenodo.4428316 (2022).
- [54] J. Thoenniss, M. Sonner, A. Lerose, and D. A. Abanin, Efficient method for quantum impurity problems out of equilibrium, *Phys. Rev. B* **107**, L201115 (2023).
- [55] N. Ng, G. Park, A. J. Millis, G. K. Chan, and D. R. Reichman, Real time evolution of Anderson impurity models via tensor network influence functionals, *Phys. Rev. B* **107**, 125103 (2023).

- [56] V. Link, H.-H. Tu, and W. T. Strunz, Open quantum system dynamics from infinite tensor network contraction, [arXiv:2307.01802](https://arxiv.org/abs/2307.01802).
- [57] H. F. Trotter, On the product of semi-groups of operators, *Proc. Am. Math. Soc.* **10**, 545 (1959).
- [58] G. Benenti, G. Casati, D. Rossini, and G. Strini, *Principles of Quantum Computation and Information: A Comprehensive Textbook* (World Scientific, Singapore, 2018).
- [59] R.-E. Plessix, A review of the adjoint-state method for computing the gradient of a functional with geophysical applications, *Geophys. J. Int.* **167**, 495 (2006).
- [60] N. Khaneja, T. Reiss, C. Kehlet, T. Schulte-Herbrüggen, and S. J. Glaser, Optimal control of coupled spin dynamics: Design of NMR pulse sequences by gradient ascent algorithms, *J. Magn. Reson.* **172**, 296 (2005).
- [61] S. D. Mishra, R. Trivedi, A. H. Safavi-Naeini, and J. Vučković, Control design for inhomogeneous-broadening compensation in single-photon transducers, *Phys. Rev. Appl.* **16**, 044025 (2021).
- [62] A. J. Leggett, S. Chakravarty, A. T. Dorsey, M. P. A. Fisher, A. Garg, and W. Zwerger, Dynamics of the dissipative two-state system, *Rev. Mod. Phys.* **59**, 1 (1987).
- [63] I. de Vega and D. Alonso, Dynamics of non-Markovian open quantum systems, *Rev. Mod. Phys.* **89**, 015001 (2017).
- [64] A. J. Ramsay, A review of the coherent optical control of the exciton and spin states of semiconductor quantum dots, *Semicond. Sci. Technol.* **25**, 103001 (2010).
- [65] A. J. Ramsay, T. M. Godden, S. J. Boyle, E. M. Gauger, A. Nazir, B. W. Lovett, A. M. Fox, and M. S. Skolnick, Phonon-induced rabi-frequency renormalization of optically driven single InGaAs/GaAs quantum dots, *Phys. Rev. Lett.* **105**, 177402 (2010).
- [66] S. Lüker, K. Gawarecki, D. E. Reiter, A. Grodecka-Grad, V. M. Axt, P. Machnikowski, and T. Kuhn, Influence of acoustic phonons on the optical control of quantum dots driven by adiabatic rapid passage, *Phys. Rev. B* **85**, 121302 (R) (2012).
- [67] R. Fletcher, *Practical Methods for Optimization*, 2nd ed. (John Wiley and Sons, New York, 2000).
- [68] P. Virtanen *et al.* (SciPy 1.0 Contributors), SciPy1.0: Fundamental algorithms for scientific computing in PYTHON, *Nat. Methods* **17**, 261 (2020).
- [69] G. C. Hegerfeldt, Driving at the Quantum speed limit: Optimal control of a two-level system, *Phys. Rev. Lett.* **111**, 260501 (2013).
- [70] G. D. Mahan, *Many-Particle Physics* (Springer Science & Business Media, New York, 2013).
- [71] L. Viola, E. Knill, and S. Lloyd, Dynamical decoupling of open quantum systems, *Phys. Rev. Lett.* **82**, 2417 (1999).
- [72] F. A. Pollock, C. Rodríguez-Rosario, T. Frauenheim, M. Paternostro, and K. Modi, Operational Markov condition for quantum processes, *Phys. Rev. Lett.* **120**, 040405 (2018).
- [73] L. Li, M. J. W. Hall, and H. M. Wiseman, Concepts of quantum non-Markovianity: A hierarchy, *Phys. Rep.* **759**, 1 (2018).
- [74] S. Wißmann, A. Karlsson, E.-M. Laine, J. Piilo, and H.-P. Breuer, Optimal state pairs for non-Markovian quantum dynamics, *Phys. Rev. A* **86**, 062108 (2012).
- [75] M. Larocca, P. M. Poggi, and D. A. Wisniacki, Quantum control landscape for a two-level system near the quantum speed limit, *J. Phys. A* **51**, 385305 (2018).
- [76] E. P. Butler, G. E. Fux, C. Ortega-Taberner, B. W. Lovett, J. Keeling, and P. R. Eastham, Zenodo, [10.5281/zenodo.10469096](https://zenodo.org/doi/10.5281/zenodo.10469096).